Cardiol Young 2005; 15 (Suppl. 3): 68–73

ISSN 1047-9511

Critical issues in studies of flow through the Fontan circuit after 10 years of investigation

Mauro Grigioni, Giuseppe D'Avenio, Costantino Del Gaudio, Umberto Morbiducci

Cardiovascular Bioengineering, Technology and Health Department, Istituto Superiore di Sanità, Rome, Italy

Keywords: Total cavopulmonary connection; computational fluid dynamics; particle image velocimetry; hydraulic power loss

Since the pioneering work of Fontan and Baudet,[1] who suggested that a dysfunctional right ventricle could be bypassed by connecting the pulmonary arteries directly to the right atrium in the so-called atriopulmonary anastomosis, much experience has been gained in the field of the functionally univentricular circulation. In view of the continuing need to optimize the fluid dynamics of the connection, research on this topic remains very active. In particular, it is relevant to consider the power dissipated during flow across a connection of this type, due to the low level of the pressure head available for perfusion. The flow to the lungs in this setting is driven only by the low pressure in the caval veins, thus making it essential to minimize the losses of energy in the connection between the terminal part of the venous system and the pulmonary arteries.

The total cavopulmonary connection is a particular surgical variant producing the Fontan circulation, in which the caval veins are anastomosed directly to the pulmonary arteries. In this review, we discuss the studies that have been done in the recent past at the Istituto Superiore di Sanità on the issue of the total cavopulmonary connection, using different techniques. An experimental characterization was carried out by means of visualization of flow with the technique of particle image velocimetry, seeking to verify the structural features of the total cavopulmonary connection with different degrees of offset between the caval veins. A numerical study was also performed, aiming at characterizing the fields of flow in the setting of unbalanced pulmonary resistances. This is representative of stenosis within the pathways, a frequent occurrence in the congenital cardiac malformations that need treatment by surgical creation of the functionally univentricular circulation. We demonstrated that computational fluid dynamics served as a capable tool to predict the fields of flow in the surgical connections under consideration, helping us to integrate the results of experiments using test models. Several researchers have previously adopted such techniques to study the complex flows arising in these kinds of anastomosis.[2–5] Lastly, we discuss the analytical approach to the determination of the power dissipated across a multiple input/output connection, which is an often overlooked problem, and can be of interest in other surgical options for the treatment of the cardiovascular disease, such as the provision of mechanical assistance to the circulation.

Correspondence to: Dr Mauro Grigioni, Cardiovascular Bioengineering, Technology and Health Department, Istituto Superiore di Sanità, Viale Regina Elena 299, 00161 Rome, Italy. Tel: +39 6 4990 2855; Fax: +39 6 4938 7079; E-mail: grigioni@iss.it

Materials and methods

We created two glassblown models of the total cavopulmonary connection at the premises of the Istituto Superiore di Sanità. These phantoms were designed on the basis of angiographic and magnetic resonance imaging data from a total of 110 patients undergoing construction of a total extracardiac cavopulmonary connection at Bambino Gesù Hospital, Rome. Such data were used to identify the two more frequently used geometric configurations of the total extracardiac cavopulmonary connection. In the first, the inferior caval venous conduit is placed leftward, with 6 millimetres offset, of the anastomosis to the superior caval vein. The inferior caval venous conduit in this pattern forms an angle of 112° with the left pulmonary artery. In the second model, the inferior caval venous conduit is directly opposite to the Glenn anastomosis. In both models, the diameters of

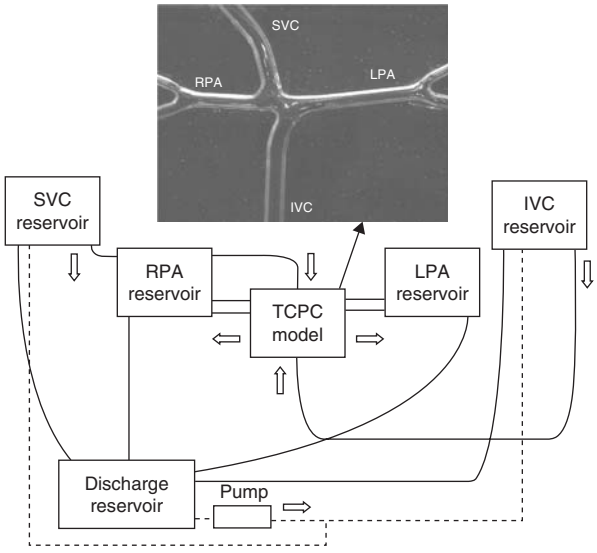

Figure 1.
Scheme of the mock loop for evaluation of the total cavopulmonary connection using fluid dynamics.

the caval veins was 11.5 millimetres, while the diameters of both pulmonary arteries was 8.6 millimetres.

The models were inserted in a steady-flow loop, in which the flow could be controlled in each branch of the connection by regulating the pressure of the corresponding outlet and inlet. We investigated four rates of flow, from 1 to 4 litres per minute, respectively. A scheme of the flow loop is presented in Figure 1, in which we also illustrate the glassblown model. Changes in pulmonary arterial resistance were simulated by narrowing the tubes connected to either pulmonary arterial branch, as described elsewhere.[6]

Visualization of flow of different selected conditions was allowed by a laser sheet and a high-speed videographic system (Kodak Ektapro), with recordings at frame rates of 50, 125, and 250 frames per second, respectively, thus providing a view of a particular condition of flow related to the optimization of the cavopulmonary connection.

Following this preliminary approach, the velocimetric assessment was done with particle imaging velocimetry, employing a Dantec 2D particle imaging velocimetry system together with a Quantel Twins Nd:YAG Q-switched laser. The Visiflow programme, for the Atomic Energy Authority, United Kingdom, was used for the analysis of the particle imaging velocimetry.

Computational model

The model we considered for numeric investigations, built by angiographic data, represents one of more frequently used geometric configurations of the total extracardiac cavopulmonary connection, and corresponded to the first model described above. A finite element technique was applied to simulate realistic dynamics in the connection, and the general purpose computational fluid dynamics code FIDAP, developed by Fluent Incorporated, from Lebanon, New Hampshire, United States of America, was used, permitting solution of the Navier–Stokes equations. The computational grid for finite elements analysis was accomplished with a hybrid mesh made of 151,000 tetrahedral cells plus about 14,150 hexahedral cells, giving a total of 46,750 nodes. Flow was assumed to be laminar. The fluid simulating blood was assumed to be homogeneous, incompressible, and newtonian, having a specific mass, ρ, equal to 1060 kilograms per metre squared, and a constant dynamic viscosity, μ, equal to 3.5×10^{-3} Pa · s. The numeric simulations were obtained under conditions of steady flow. The walls of vessels were assumed to be rigid, and no condition for slip was imposed. A parabolic profile for rate of flow was imposed at the inferior and superior caval veins for a total rate of flow of 3 litres per minute, being distributed with a ratio of 3 to 2 between the inferior and superior veins.

The numerical study allowed us to consider the effect of unbalanced pulmonary arterial resistances. Pulmonary arterial load was simulated with the imposition of three sets of boundary conditions for the pressure. We investigated the effects of balanced resistances between the right and left pulmonary arteries, and two unbalanced resistances, choosing a difference in pressures equal to either plus or minus 2 millimetres of mercury.

The issue of loss of energy

Another aspect of the Fontan circulation that deserves careful consideration is the question of the dissipation of power across the connection itself. This issue is subjected to potential sources of errors, frequently overlooked. It is usually assumed,[7] that

$$W_{\text{loss}} = \sum_{i=1}^{m_{\text{IN}}} p_i Q_i - \sum_{j=1}^{m_{\text{OUT}}} p_j Q_j + \frac{\rho}{2} \sum_{i=1}^{m_{\text{IN}}} U_i^2 Q_i - \frac{\rho}{2} \sum_{j=1}^{m_{\text{OUT}}} U_j^2 Q_j \qquad (1)$$

or, in compact form, $W_{\text{loss}} = W_{\text{stat}} + W_{\text{dyn}}$, sum of the contribution due to the static pressures and the dynamical pressures.

In these formulas, p_i, Q_i, U_i represent the static pressure, rate of flow, and mean velocity in the section k, respectively, and m_{IN} (m_{OUT}) is the number of inlet (outlet) ports of the connection.

Equation (1) is potentially affected by oversimplified calculations. As has been suggested,[8] a more general formula should be considered, which is derived from the energy equation for a Lagrangian

https://doi.org/10.1017/S1047951105001678 Published online by Cambridge University Press

fluid element. The integration of the rate of dissipation of energy, as irrecoverable heat through fluid friction, over a given control volume, bounded by inlet and outlet sections as well as by the vascular walls, yields the dissipation of power. Omitting the minute details of the derivation of the reassessed formula for power dissipation, it is worth considering that the two main effects usually neglected are, first, the fact that the piezometric pressure $p + \rho g h$ must be considered instead of the static pressure p, in each outflow/inflow section of the total cavopulmonary connection, and second, the influence of the flow profile in each section, which affects the value of the average of Q^3, so that usually the following inequality holds:

$$\overline{Q}^3 \neq (\overline{Q})^3$$

where the overbar denotes spatial averaging over the section. The usual formula, instead, is derived by setting, implicitly, $\overline{Q^3} \neq (\overline{Q})^3$.

A final corrected form of power dissipation is the following:

$$W_{\text{loss}} = \sum_{i=1}^{m_{\text{IN}}} p_i^* Q_i - \sum_{j=1}^{m_{\text{OUT}}} p_j^* Q_j + \frac{\rho}{2} \int_{\text{IN}} u^3 dA - \frac{\rho}{2} \int_{\text{OUT}} u^3 dA$$
$$= \sum_{i=1}^{m_{\text{IN}}} p_i^* Q_i - \sum_{j=1}^{m_{\text{OUT}}} p_j^* Q_j + \frac{\rho}{2} \sum_{i=1}^{m_{\text{IN}}} \beta_i U_i^2 Q_i - \frac{\rho}{2} \sum_{j=1}^{m_{\text{OUT}}} \beta_j U_j^2 Q_j, \quad (2)$$

which, as well as in Eqn (1), has the form $W_{\text{loss}} = W_{\text{stat}} + W_{\text{dyn}}$.

In the second equation, p_i^* is defined as the piezometric pressure (or $p^* = p + \rho g h$), and β_i represents the ratio between the average of the cube of the velocity and the cube of the average of the velocity in the section i. In the following section, the contributions W_{stat} and W_{dyn} to the power dissipated across a total cavopulmonary connection will be considered according to the approaches given by the two equations.

Results and discussion

The flow field relative to a restricted artery, corresponding to a stenosed right pulmonary artery, is shown in Figure 2. In the case of equal divisions of flow between the caval veins, the stenosed right pulmonary artery, carrying three-tenths of the total flow to the lungs, as a model of enhanced arterial resistance, caused a redirection of the flow through the superior caval vein also towards the left pulmonary artery. This contrasts with the usual situation in which preferential flow is to the right pulmonary artery, as typically occurs with normal pulmonary arterial resistances. As reported elsewhere,[9] this type of total cavopulmonary connection normally presents a large central structure, that acts as a regulator to provide smooth fields of flow without excessive losses of power (Fig. 3). This "vortex", which was called beneficial vortex because it is not associated with high pressure losses, is seen to disappear in Figure 2 when the pulmonary resistances are unbalanced. The flows through both caval veins contribute to the flow through the normally patent pulmonary arteries. Similar conditions were obtained when we simulated stenosis of the left pulmonary artery. No evidence of

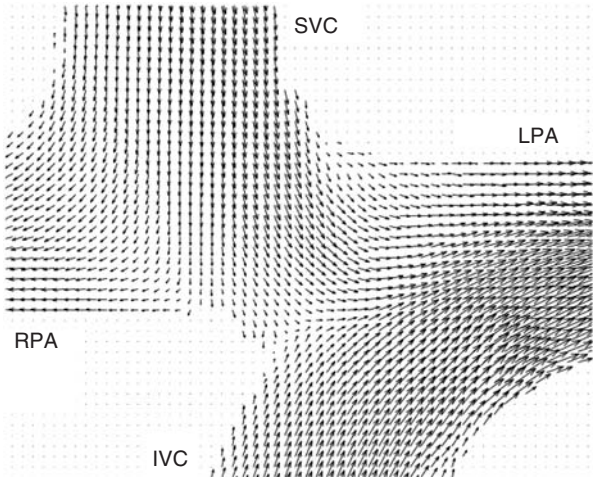

Figure 2.
Fields of flow obtained using particle image velocimetry to study the total cavopulmonary connection as modelled with stenosis of the right pulmonary artery.

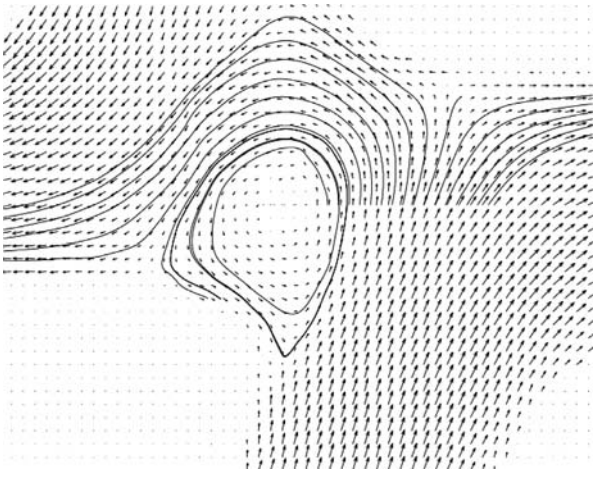

Figure 3.
Comparable studies of particle image velocimetric analysis of the fields of flow in the total cavopulmonary connection with offset between the caval veins, but with balanced resistances in the pulmonary arteries. A number of streamlines, starting from a horizontal segment intersecting the centre of the vortex, have been superimposed in order to show the circulation in the connection.

https://doi.org/10.1017/S1047951105001678 Published online by Cambridge University Press

large separation of flows is given by the velocity vector maps provided for these latter conditions.

These features of the Fontan circulation must be considered at the time of catheterization if the optimal design is to be chosen for the surgical intervention, taking into account the structure of the pulmonary arteries, and remembering the frequent occurrence of abnormal pathologies in the young patients considered for operation.

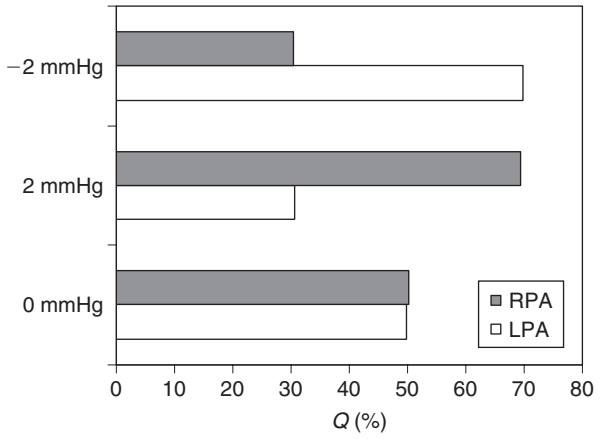

Figure 4.
Distributions of the rates of flow in the total cavopulmonary connection for three investigated pressure differences in the pulmonary arteries with a total rate of flow of 3 litres per minute.

The numerical simulations provide strong support for the experimental evaluations of different surgical connections. In Figure 4, we show the division in the rates of flow in the pulmonary arteries in the case of the topological connection selected at Bambino Gesù Hospital. The distribution of the flows of 3 litres per minute entering from the caval veins between the two pulmonary arteries is strongly dependant on the arterial load. When unbalanced, this causes a significant redistribution of the venous blood in the pulmonary tree. The three-dimensional morphology of the axial profiles of velocity in the pulmonary arteries is shown in Figure 5 for all the investigated conditions. When the resistances in the pulmonary arteries were balanced, there was a quite skewed morphology of the profiles of axial velocity with respect to the typical Poiseuillan parabolic velocity profile, with

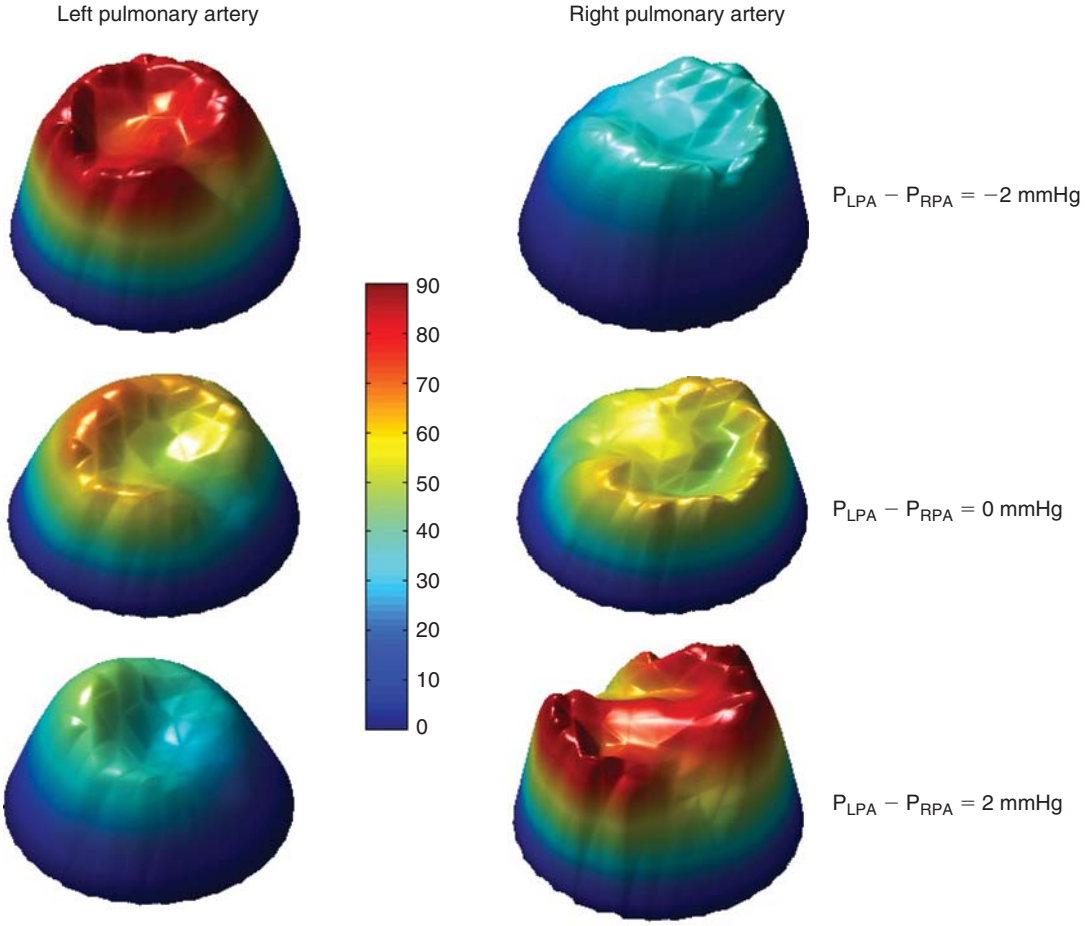

Figure 5.
Three-dimensional axial velocity profiles in the left pulmonary artery, 5.5 centimetres from the axis of the superior caval vein, and in the right pulmonary artery 3.5 centimetres from the axis of the superior caval vein.

https://doi.org/10.1017/S1047951105001678 Published online by Cambridge University Press

no relevant differences in magnitude. This situation was different when the resistances were unbalanced. The imposed resistances to flow in the pulmonary arteries caused a large variation in the magnitude of velocity, with a consequent redistribution of the relative flows in these vessels. Moreover, the morphology of the axial profiles of velocity highlighted a less skewed configuration in the vessel with the higher resistance.

Considering the theoretical issue of the dissipation of power, in Figure 6 we report the static contribution W_{static} to the dissipation according to the two approaches under consideration, and as represented by the first two terms in our two equations. The two formulas yield a substantial difference in the case of the model of the total cavopulmonary connection model with the axis of the caval veins lying on a vertical plane, due to the effect of the different mean heights chosen for the vessels comprising the total cavopulmonary connection. The evaluation of the difference in the dynamic contribution was carried out with some approximations, due to the incomplete knowledge about the local flow filed in the IN/OUT sections. If the flow at the entrance of the pulmonary arteries was assumed to be perfectly flat, we are able to model the profile of flow with the generalized Poiseuille formula:

$$u(r) = u_0\left[1 - \left(\frac{r}{R}\right)^n\right] \qquad (3)$$

where n represents an index of bluntness, and a flat profile corresponds to $n = \infty$. At the section of the measurements, 20 millimetres downstream of the centre of the cross, we computed the value of n according to an analytical interpolation of the values on n corresponding to the plug flow at the entrance of the vessel and the Poiseuillian profile, reached after the length of the entrance at the considered rate of flow. Instead, in the caval veins, we assumed the profile of flow to be Poiseuillian, owing to the distance travelled by the fluid upstream of the sections in the veins. Then, the dynamical contribution according to Eqn (2) was plotted in Figure 7, along with the same contribution provided by Eqn (1). The difference in the two quantities is remarkable, since the values of n were found to be very high in the pulmonary arteries. It must be underlined, however, that a perfectly flat profile of flow at the entrance of the pulmonary artery has been a simplifying assumption, while the low velocities from the caval veins give the possibility to assume parabolic like profiles. Due to the fact that the flow in the right pulmonary artery has its predominant contribution from the superior caval vein, while conversely the flow from the inferior caval

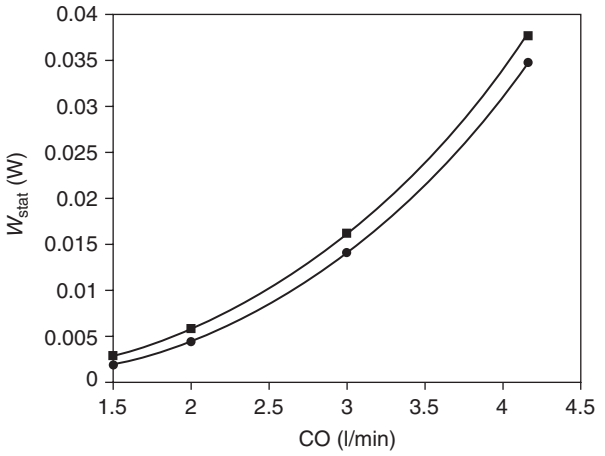

Figure 6.
The static contribution (W_{stat}) to the power dissipated in the total cavopulmonary connection, according to Eqn (1) as shown in the text, and to the proposed method using the first two terms in Eqn (2). The respective markers are circles and squares.

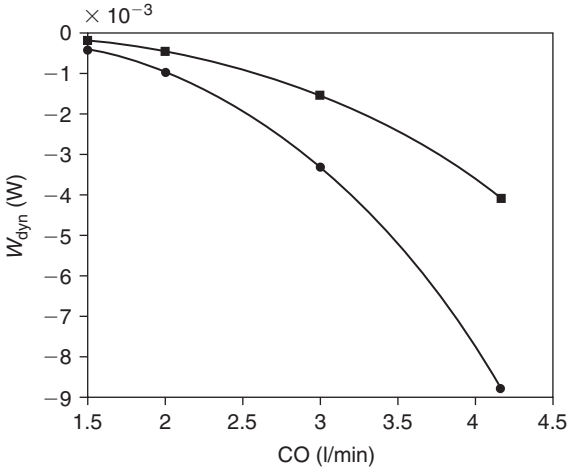

Figure 7.
The dynamic contribution (W_{dyn}) to the power dissipated in the total cavopulmonary connection, according to the usual Eqn (1), and to our proposed method using the last two terms in Eqn (2). The respective markers are circles and squares.

vein is directed predominantly to the left pulmonary artery, the profiles of flow in the right pulmonary artery are more skewed than those in the left pulmonary artery.[10,11] In the latter case, the value of β should accordingly be calculated by means of the last two terms in Eqn (2), thus taking account of the correct value of W_{dyn}.

In Figure 8, finally, the total power loss $W_{\text{loss}} = W_{\text{stat}} + W_{\text{dyn}}$ is shown. The dissipation of power according to this more accurate approach is larger than W_{loss}, as given in Eqn (1). This difference could

https://doi.org/10.1017/S1047951105001678 Published online by Cambridge University Press

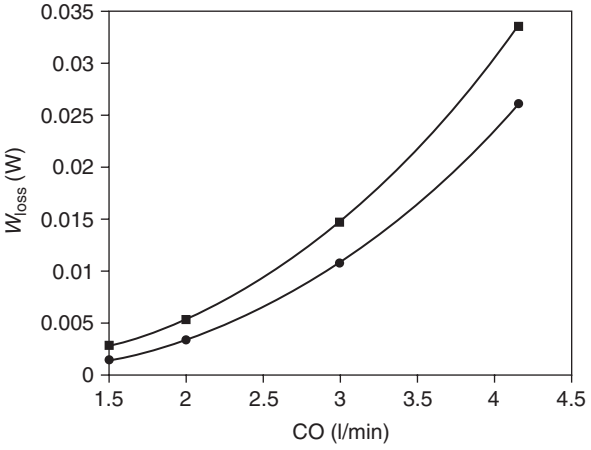

Figure 8.
The total dissipated power (W_{loss}) in the total cavopulmonary connection according to the usual Eqn (1), and our proposed method using Eqn (2). The respective markers are circles and squares.

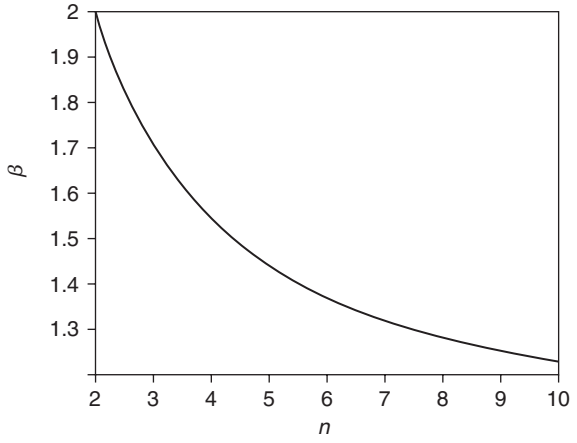

Figure 9.
The correction factor β*, to be employed in Eqn (2), as a function of the index of bluntness* n *in each section of the control volume.*

well be relevant should such equations be used to predict future outcomes over the period of follow up.

Figure 9 reports the relationship between the correction factor β_i used in Eqn (2) and the bluntness index n, relative to the generalized Poiseuille formula shown in Eqn (3). It is apparent how the usual, implicit, choice of $\beta_i = 1$ corresponds to a perfectly flat flow profile. This finding, however, is an infrequent condition in the circulation, especially in the venous return.

Conclusions

Our experimental and numerical investigations on the fluid dynamics and hydraulic features of the total cavopulmonary connection have allowed us to develop a critical background, and to make inference concerning the spatial arrangement of this connection that can guarantee the best outcome for children with functionally univentricular hearts. Visualization of flow, and particle image velocimetry, in glass blown phantoms led to the identification of a peculiar vortical structure, the so-called beneficial vortex,[9] that is produced by a specific anastomosis of the inferior caval vein relative to the pulmonary arteries, and which helps for an efficient hydraulic performance and pulmonary perfusion. Moreover, computational fluid dynamics were shown to function as a complementary tool to predict and visualize fluid dynamic structures that could not easily be evaluated from the experimental studies, also giving the possibility to modify the investigated geometric connection whilst avoiding the necessity to alter a more complex in vitro experimental set-up. As a consequence, results obtained over the last 10 years by the Istituto Superiore di Sanità assured a scientific collaboration with Bambino Gesù Hospital that led to continuous critical discussions in the assessment of this surgical procedure and its innovative design.

References

1. Fontan F, Baudet E. Surgical repair of tricuspid atresia. Thorax 1971; 26: 240–248.
2. de Leval MR, Dubini G, Migliavacca F, et al. Use of computational fluid dynamics in the design of surgical procedures: application to the study of competitive flows in cavopulmonary connections. J Thorac Cardiovasc Surg 1996; 111: 502–513.
3. Bolzon G, Pedrizzetti G, Grigioni M, Zovatto L, Daniele C, D'Avenio G. Flow on the simmetry plane of a total cavopulmonary connection. J Biomech 2002; 35: 595–608.
4. Pekkan K, de Zelicourt D, Ge L, et al. Physics-driven CFD modeling of complex anatomical cardiovascular flows – a TCPC case study. Ann Biomed Eng 2005; 33: 284–300.
5. DeGroff C, Birnbaum B, Shandas R, Orlando W, Hertzberg J. Computational simulations of the total cavo-pulmonary connection: insights in optimizing numerical solutions. Med Eng Phys 2005; 27: 135–146.
6. Grigioni M, Amodeo A, Daniele C, D'Avenio G, Formigari R, Di Donato RM. Particle image velocimetry analysis of the flow field in the total cavopulmonary connection. Artif Organs 2000; 24: 946–952.
7. Sharma S, Goudy S, Walker P, et al. In vitro flow experiments for determination of optimal geometry of total cavopulmonary connection for surgical repair of children with functional single ventricle. J Am Coll Cardiol 1996; 27: 1264–1269.
8. Leefe SE, Gentle CR. Theoretical evaluation of energy loss methods in the analysis of prosthetic heart valves. J Biomed Eng 1987; 9: 121–127.
9. Amodeo A, Grigioni M, Oppido G, et al. The beneficial vortex and best spatial arrangement in total extracardiac cavopulmonary connection. J Thorac Cardiovasc Surg 2002; 124: 471–478.
10. He X, Ku DN. Pulsatile flow in the human left coronary artery bifurcation: average conditions. J Biomech Eng 1996; 118: 74–82.
11. Naruse T, Tanishita K. Large curvature effect on pulsatile entrance flow in a curved tube: model experiment simulating blood flow in an aortic arch. J Biomech Eng 1996; 118: 180–186.

https://doi.org/10.1017/S1047951105001678 Published online by Cambridge University Press